



PERGAMON

International Journal of Solids and Structures 38 (2001) 7999–8018

INTERNATIONAL JOURNAL OF  
**SOLIDS and**  
**STRUCTURES**

[www.elsevier.com/locate/ijsolstr](http://www.elsevier.com/locate/ijsolstr)

# Parameter estimation of hyperelasticity relations of generalized polynomial-type with constraint conditions

Stefan Hartmann \*

*Institute of Mechanics, University of Kassel, Mönchebergstrasse 7, 34109 Kassel, Germany*

Received 1 June 2000; in revised form 20 December 2000

---

## Abstract

In this article the identification of the material parameters occurring in isotropic and incompressible hyperelasticity relations of generalized polynomial-type is discussed. The underlying strain-energy function depends on the first and second invariant of the left Cauchy–Green tensor in the form of a polynomial. The material parameters are the polynomial coefficients. This leads in several identification processes to linear least-square problems. However, in most applications the parameters are not restricted to a range of validity. This article points out that the assumption of merely positive material parameters leads to a non-negative strain-energy function in any process which is underpinned by requirements with respect to gradient and convexity behaviour in certain deformations. Furthermore, it is shown that for positive material parameters no non-monotonic behaviour occurs in simple deformation processes under consideration outside the identification region. The second topic of the article deals with some identification applications of tension–torsion tests, which are carried out by Haupt and Sedlan (Archive of Applied Mechanics, 2000), taking into account the inequality constraints emphasized. Under certain assumptions, this naturally leads to new, specific models. Furthermore, it is shown that the parameter estimation becomes much less sensitive than in the unconstrained case. © 2001 Elsevier Science Ltd. All rights reserved.

**Keywords:** Hyperelasticity; Parameter identification; Tension–torsion; Least-square method

---

## 1. Introduction

Since the work of Rivlin and Saunders (1951), which assumed a strain-energy function of the form

$$\psi(\mathbf{I}_{\mathbf{B}}, \mathbf{II}_{\mathbf{B}}) = \sum_{i=0}^m \sum_{j=0}^n c_{ij} (\mathbf{I}_{\mathbf{B}} - 3)^i (\mathbf{II}_{\mathbf{B}} - 3)^j, \quad (1)$$

a variety of constitutive models incorporated in this class of strain energy function have been proposed for incompressible materials. Here,  $\mathbf{I}_{\mathbf{B}} = \text{tr} \mathbf{B} = B_i^i$  symbolize the first and  $\mathbf{II}_{\mathbf{B}} = 1/2((\text{tr} \mathbf{B})^2 - \text{tr} \mathbf{B}^2)$  and second invariant of the left Cauchy–Green tensor  $\mathbf{B} = \mathbf{F} \mathbf{F}^T$ , with the deformation gradient  $\mathbf{F} = \text{GRAD} \vec{\chi}_{\mathbf{R}}(\vec{\mathbf{X}}, t)$ .

---

\* Tel.: +49-561-804-2719; fax: +49-561-804-2720.

E-mail address: [hart@ifm.maschinenbau.uni-kassel.de](mailto:hart@ifm.maschinenbau.uni-kassel.de) (S. Hartmann).

Table 1

Material models based on polynomial order

References	Coefficients used								
Mooney–Rivlin*	$c_{10}$	$c_{01}$							
James et al. (1975)	$c_{10}$	$c_{01}$	$c_{11}$	$c_{20}$	$c_{02}$				
James et al. (1975)	$c_{10}$	$c_{01}$	$c_{11}$	$c_{20}$	$c_{02}$	$c_{21}$	$c_{12}$	$c_{30}$	$c_{03}$
Isihara et al. (1951)	$c_{10}$	$c_{01}$		$c_{20}$					
Neo–Hooke**	$c_{10}$								
James et al. (1975)	$c_{10}$	$c_{01}$	$c_{11}$	$c_{20}$				$c_{30}$	
James et al. (1975)	$c_{10}$	$c_{01}$	$c_{11}$	$c_{20}$	$c_{02}$	$c_{21}$		$c_{30}$	$c_{40}$
Biderman (1958)	$c_{10}$	$c_{01}$		$c_{20}$				$c_{30}$	
Tschoegl (1971)	$c_{10}$	$c_{01}$	$c_{11}$						
Tschoegl (1971)	$c_{10}$	$c_{01}$					$c_{22}$		
Lion (1997)	$c_{10}$	$c_{01}$							$c_{50}$
Haupt and Sedlan (2001)	$c_{10}$	$c_{01}$	$c_{11}$		$c_{02}$			$c_{30}$	

\* See Mooney (1940); Rivlin (1948).

\*\* See Rivlin (1948).

$\vec{x} = \vec{\chi}_R(\vec{X}, t)$  denotes the motion of a particle  $\vec{X}$ . These models are widely used in theoretical and practical applications, e.g. finite element calculations. The identification of the material parameters  $c_{ij}$  is usually carried out by means of experiments for homogeneous stress–strain states (simple tension, simple or pure shear, biaxial tension) or inhomogeneous deformations (tension–torsion tests) for which analytical solutions exist. These solutions depend linearly on the material parameters which, in the case of their identification, leads to a linear least-square problem. Table 1 summarizes a number of models known from the literature. The most well-known elasticity relations are the Neo–Hooke model,  $\psi(I_B) = c_{10}(I_B - 3)$ , and the Mooney–Rivlin model,  $\psi(I_B, II_B) = c_{10}(I_B - 3) + c_{01}(II_B - 3)$  (see Mooney, 1940; Rivlin, 1948). The material parameters of both models must be positive,  $c_{01} \geq 0$ ,  $c_{10} > 0$ , to satisfy the requirement of a positive strain-energy (see, for example, Truesdell and Noll, 1965, Section 95; or Haupt, 2000, Ch. 9.2.4). However, in the case of higher-order models, no generally accepted requirement exists, instead, one might be afraid to exclude possible solution if all parameters are positive. This is underpinned by identification processes which, with negative coefficients, yield very good adaptations of the model to the experimental data. However, outside the identification region the stress–strain curves may give non-physical responses, for example, for positive stretches in a tensile test negative stresses occur (see, for example, James et al., 1975; or Hartmann, 2001). In Hartmann (2001) numerical studies applied to tension–torsion tests are carried out in order to obtain a better insight into the sensitivity of the identification processes. As a result, it is mentioned that higher-order models are most sensitive with respect to small changes of the test data. However, in all these studies negative material parameters cannot be ruled out for either a small or a high number of test data.

In order to avoid the phenomena of non-monotonic stress–strain curves, Kao and Razgunas (1986) introduced some non-linear inequality constraint conditions which must be satisfied by the material parameters  $c_{ij}$  in the case of models 2 and 6 of Table 1. These constraints do not exclude negative parameters and are developed on the basis of simple tension tests so that physically plausibles curves are obtained. However, it is possible to obtain material parameters satisfying these inequality constraints but leading to non-physical curves in other tests (e.g. simple shear). Further investigations concerning the identification of the material parameters under constraint conditions, resulting from the restriction of a stability criterion, have been carried out by Przybylo and Arruda (1998). They make use of a certain form of the Drucker stability inequality cited in Johnson et al. (1994) to the theory manual of the finite element code ABAQUS (see, for example, Hibbit et al., 1998). Przybylo and Arruda (1998) and Johnson et al. (1994) assume the constraint  $\sum_{i=1}^3 d\sigma_i d\epsilon_i > 0$  with the increments of the principal Cauchy stresses  $\sigma_i$  and a non-specified

principal strain-increment  $d\epsilon_i$ . The strain increments are defined in Hibbitt et al. (1998) by the increment of the logarithmic strains,  $d(\ln \lambda_i)$ , where the  $\lambda_i$ 's are the principal stretches. All these investigations are restricted to plane stress problems ( $\sigma_3 = 0$ , i.e. simple tension, pure shear and biaxial tension) because in that case it is possible to eliminate the undetermined pressure of the Cauchy stresses. In their study they arrive at positive material parameters  $c_{ij} > 0$  and further non-linear inequality constraints. The investigations mentioned above remind one of Hill's inequality, in which the scalar product of an objective stress-rate and strain-rate must be positive to characterize a stable material. A detailed discussion on necessary conjugate or dual stress and strain-rate tensors is carried out by Hill (1970) and Haupt and Tsakmakis (1996) and is treated by Ogden (1984) with respect to constitutive inequalities. In the case of incompressibility only one pair of stress-rate and strain-rate tensors yields an inequality,  $w_{\text{incr}} = \dot{\mathbf{T}}^{(0)} \cdot \dot{\mathbf{E}}^{(0)} > 0$ , without specifying the pressure  $p$ , namely  $\mathbf{T}^{(0)} = \mathbf{R}^T \mathbf{T} \mathbf{R}$  and  $\mathbf{E}^{(0)} = \ln \mathbf{U}$ , where  $\mathbf{T}$  defines the Cauchy stress tensor,  $\mathbf{R}$  the rotation tensor of the polar decomposition of the deformation gradient and  $\mathbf{U}$  the right stretch tensor (Ogden, 1984, Ch. 6.2.8). The dot denotes the material time derivative. However, the fulfillment of  $w_{\text{incr}} > 0$  is an awkward task leading to complicated non-linear constraints.

In contrast to the investigations mentioned above we propose in this article that all material parameters of any kind of strain energy function (1) should be positive, since the fundamental requirement of an always positive strain-energy function in all ranges of deformation is easily fulfilled. This, somewhat restrictive assumption may exclude possible strain-energy functions. However, without particular investigations of some specific models this assumption leads to physically plausible results in the simple deformation tests examined. In order to show this, we first investigate the gradient behaviour of simple tension, simple shear, biaxial tension and pure torsion tests. Furthermore, the Baker–Ericksen inequality, which characterizes a specific stability behaviour, is satisfied. This also happens, as a sufficient condition, if all material parameters are positive (Truesdell and Noll, 1965).

The consequence of the assumption of positiveness leads to a linear least-square problem with non-negative solution, i.e. linear inequality constraints exist for the material parameters. In contrast to the investigations of the parameter estimations performed in Hartmann (2001), the incorporation of the inequality constraints is studied in this article. To gain a better insight with respect to the consequences in the parameter estimation, the identification of the material parameters is carried out utilizing tension–torsion test published by Haupt and Sedlan (2001).

## 2. Basic assumptions and simple deformations

First of all, the strain-energy function (1) is investigated. Eq. (1) is rewritten in terms of the singular values  $\lambda_i > 0$ ,  $i = 1, 2, 3$ , of the deformation gradient  $\mathbf{F} = \sum_{i=1}^3 \lambda_i \vec{v}_i \otimes \vec{u}_i$ , i.e. the eigenvalues  $\lambda_i$  of the right or left stretch tensor  $\mathbf{U} = \sum_{i=1}^3 \lambda_i \vec{u}_i \otimes \vec{u}_i$  or  $\mathbf{V} = \sum_{i=1}^3 \lambda_i \vec{v}_i \otimes \vec{v}_i$  respectively, where  $\vec{u}_i$  and  $\vec{v}_i$  are the eigenvectors of  $\mathbf{U}$  and  $\mathbf{V}$ . Both tensors result from the polar decomposition  $\mathbf{F} = \mathbf{R} \mathbf{U} = \mathbf{V} \mathbf{R}$  with the rotation tensor  $\mathbf{R}$ . First, we evaluate the left Cauchy–Green tensor  $\mathbf{B} = \mathbf{F} \mathbf{F}^T = \sum_{i=1}^3 \lambda_i^2 \vec{v}_i \otimes \vec{v}_i$ . If the incompressibility condition  $\det \mathbf{B} = \lambda_1^2 \lambda_2^2 \lambda_3^2 = 1$  is taken into account, it is easy to show that

$$I_{\mathbf{B}} = \text{tr } \mathbf{B} = \lambda_1^2 + \lambda_2^2 + \lambda_3^2 = \lambda_1^2 + \lambda_2^2 + \frac{1}{(\lambda_1 \lambda_2)^2} \quad (2)$$

and

$$II_{\mathbf{B}} = \frac{1}{2} ((\text{tr } \mathbf{B})^2 - \text{tr } \mathbf{B}^2) = \text{tr } \mathbf{B}^{-1} = \frac{1}{\lambda_1^2} + \frac{1}{\lambda_2^2} + \frac{1}{\lambda_3^2} \quad (3)$$

$$II_{\mathbf{B}} = \lambda_1^2 \lambda_2^2 + \lambda_2^2 \lambda_3^2 + \lambda_3^2 \lambda_1^2 = \lambda_1^2 \lambda_2^2 + \frac{1}{\lambda_1^2} + \frac{1}{\lambda_2^2} \quad (4)$$

hold. The strain-energy function (1) now reads in terms of the singular values

$$\psi(\mathbf{I}_B, \mathbf{II}_B) = \sum_{i=0}^m \sum_{j=0}^n c_{ij} \left( \lambda_1^2 + \lambda_2^2 + \frac{1}{\lambda_1^2 \lambda_2^2} - 3 \right)^i \left( \lambda_1^2 \lambda_2^2 + \frac{1}{\lambda_1^2} + \frac{1}{\lambda_2^2} - 3 \right)^j. \quad (5)$$

It is well-known that both parentheses are non-negative in the case of incompressibility. Nevertheless a short proof is given in Appendix B.

Keeping these results in mind, we investigate few homogeneous and inhomogeneous deformation processes, namely simple tension, simple shear, biaxial tension and pure torsion, with respect to the relation between external forces and prescribed deformational parameters. Investigations are carried out to see whether the resulting curves could be non-monotonic in the case of positive material parameters  $c_{ij}$ . In order to avoid duplicate derivations we start with the biaxial test and continue with simple shear and tension–torsion tests.

The constitutive equation

$$\mathbf{T} = -p\mathbf{I} + \varphi_1(\mathbf{I}_B, \mathbf{II}_B)\mathbf{B} - \varphi_2(\mathbf{I}_B, \mathbf{II}_B)\mathbf{B}^{-1} \quad (6)$$

forms the basis of all these cases, with the Cauchy stress tensor  $\mathbf{T}$ , which is decomposed into the pressure term  $-p\mathbf{I}$  and the so-called extra stresses  $\mathbf{S} = p\mathbf{I} + \mathbf{T}$  determined by the constitutive equations. The pressure  $p$  has to be solved by the underlying equilibrium and boundary conditions. The scalar functions  $\varphi_1(\mathbf{I}_B, \mathbf{II}_B)$  and  $\varphi_2(\mathbf{I}_B, \mathbf{II}_B)$  result from the strain-energy function (1)

$$\varphi_1(\mathbf{I}_B, \mathbf{II}_B) = 2 \frac{\partial \psi}{\partial \mathbf{I}_B} = 2 \sum_{i=1}^m \sum_{j=0}^n c_{ij} i(\mathbf{I}_B - 3)^{i-1} (\mathbf{II}_B - 3)^j \geq 0, \quad (7)$$

$$\varphi_2(\mathbf{I}_B, \mathbf{II}_B) = 2 \frac{\partial \psi}{\partial \mathbf{II}_B} = 2 \sum_{i=0}^m \sum_{j=1}^n c_{ij} j(\mathbf{I}_B - 3)^i (\mathbf{II}_B - 3)^{j-1} \geq 0, \quad (8)$$

which are obviously non-negative, since the material parameters are assumed to be non-negative and the terms  $\mathbf{I}_B - 3$  and  $\mathbf{II}_B - 3$  are non-negative. For the following calculations we need the derivatives

$$\varphi_{11}(\mathbf{I}_B, \mathbf{II}_B) = \frac{\partial \varphi_1}{\partial \mathbf{I}_B} = 2 \frac{\partial^2 \psi}{\partial \mathbf{I}_B^2} = 2 \sum_{i=2}^m \sum_{j=0}^n c_{ij} i(i-1)(\mathbf{I}_B - 3)^{i-2} (\mathbf{II}_B - 3)^j \geq 0, \quad (9)$$

$$\varphi_{22}(\mathbf{I}_B, \mathbf{II}_B) = \frac{\partial \varphi_2}{\partial \mathbf{II}_B} = 2 \frac{\partial^2 \psi}{\partial \mathbf{II}_B^2} = 2 \sum_{i=0}^m \sum_{j=2}^n c_{ij} j(j-1)(\mathbf{I}_B - 3)^i (\mathbf{II}_B - 3)^{j-2} \geq 0, \quad (10)$$

$$\varphi_{12}(\mathbf{I}_B, \mathbf{II}_B) = \frac{\partial \varphi_1}{\partial \mathbf{II}_B} = 2 \frac{\partial^2 \psi}{\partial \mathbf{I}_B \partial \mathbf{II}_B} = 2 \sum_{i=1}^m \sum_{j=1}^n c_{ij} i j (\mathbf{I}_B - 3)^{i-1} (\mathbf{II}_B - 3)^{j-1} \geq 0, \quad (11)$$

$$\varphi_{21}(\mathbf{I}_B, \mathbf{II}_B) = \frac{\partial \varphi_2}{\partial \mathbf{I}_B} = 2 \frac{\partial^2 \psi}{\partial \mathbf{II}_B \partial \mathbf{I}_B} = \varphi_{12}(\mathbf{I}_B, \mathbf{II}_B) \geq 0 \quad (12)$$

which are obviously non-negative in view of the arguments given above. Even higher derivatives, for example  $\varphi_{112} = \partial^2 \varphi_1 / \partial \mathbf{I}_B \partial \mathbf{II}_B = 2 \partial^3 \psi / \partial \mathbf{I}_B^2 \partial \mathbf{II}_B$  are non-negative.

## 2.1. Biaxial tension

A very frequently used finite deformation process is based on a plane rubber sheet loaded independently in two directions (Rivlin and Saunders, 1951; James et al., 1975). The deformation  $\vec{x} = \vec{\chi}_R(\vec{X}, t) = \lambda_1 X_1 \vec{e}_1 + \lambda_2 X_2 \vec{e}_2 + (\lambda_1 \lambda_2)^{-1} X_3 \vec{e}_3$  yields the deformation gradient  $\mathbf{F}$  and the left Cauchy–Green tensor  $\mathbf{B} = \mathbf{F} \mathbf{F}^T$ :

$$\mathbf{F} = \lambda_1 \vec{\mathbf{e}}_1 \otimes \vec{\mathbf{e}}_1 + \lambda_2 \vec{\mathbf{e}}_2 \otimes \vec{\mathbf{e}}_2 + (\lambda_1 \lambda_2)^{-1} \vec{\mathbf{e}}_3 \otimes \vec{\mathbf{e}}_3, \quad (13)$$

$$\mathbf{B} = \lambda_1^2 \vec{\mathbf{e}}_1 \otimes \vec{\mathbf{e}}_1 + \lambda_2^2 \vec{\mathbf{e}}_2 \otimes \vec{\mathbf{e}}_2 + (\lambda_1 \lambda_2)^{-2} \vec{\mathbf{e}}_3 \otimes \vec{\mathbf{e}}_3. \quad (14)$$

The invariants of the left Cauchy–Green tensor are given by Eqs. (2) and (3). Due to the structure of the left Cauchy–Green tensor (14) and the stress boundary condition  $\sigma_3 = 0$  the Cauchy stress tensor (6) acquires the form  $\mathbf{T} = \sigma_1 \vec{\mathbf{e}}_1 \otimes \vec{\mathbf{e}}_1 + \sigma_2 \vec{\mathbf{e}}_2 \otimes \vec{\mathbf{e}}_2$ . The stress coefficients are calculable via

$$\sigma_1 = -p + \varphi_1 \lambda_1^2 - \varphi_2 \lambda_1^{-2}, \quad \sigma_2 = -p + \varphi_1 \lambda_2^2 - \varphi_2 \lambda_2^{-2}, \quad (15)$$

by exploitation of the pressure  $p$  using the above-mentioned stress boundary condition in out-of-plane direction,  $\sigma_3 = 0$ . The normal forces  $N_1$  and  $N_2$ , which belong to the areas  $A_1$  and  $A_2$  in the reference configuration, yield the engineering stresses  $T_{R11} = N_1/A_1$  and  $T_{R22} = N_2/A_2$ .  $T_{R11}$  and  $T_{R22}$  are the components of the first Piola–Kirchhoff stress tensor,  $\mathbf{T}_R = \mathbf{T}\mathbf{F}^{-T}$ , i.e. we arrive at

$$\frac{N_1}{A_1} = T_{R11} = \frac{\sigma_1}{\lambda_1} = \left( \lambda_1 - \frac{1}{\lambda_1^3 \lambda_2^2} \right) (\varphi_1 + \lambda_2^2 \varphi_2), \quad (16)$$

$$\frac{N_2}{A_2} = T_{R22} = \frac{\sigma_2}{\lambda_2} = \left( \lambda_2 - \frac{1}{\lambda_1^2 \lambda_2^3} \right) (\varphi_1 + \lambda_1^2 \varphi_2) \quad (17)$$

(see, for example, Atkin and Fox, 1980, Ch. 3.5). Now, in a diagram  $T_{R11}(\lambda_1)$  the gradient behaviour for constant  $\lambda_2$  is investigated. To this end Eq. (16) is differentiated with respect to  $\lambda_1$ :

$$\begin{aligned} \frac{\partial T_{R11}}{\partial \lambda_1} &= \left( 1 + \frac{3}{\lambda_1^4 \lambda_2^2} \right) (\varphi_1 + \lambda_2^2 \varphi_2) + \left( \lambda_1 - \frac{1}{\lambda_1^3 \lambda_2^2} \right) \left( \frac{\partial \varphi_1}{\partial \mathbf{I}_B} \frac{\partial \mathbf{I}_B}{\partial \lambda_1} + \frac{\partial \varphi_1}{\partial \mathbf{II}_B} \frac{\partial \mathbf{II}_B}{\partial \lambda_1} + \lambda_2^2 \left( \frac{\partial \varphi_2}{\partial \mathbf{I}_B} \frac{\partial \mathbf{I}_B}{\partial \lambda_1} \right. \right. \\ &\quad \left. \left. + \frac{\partial \varphi_2}{\partial \mathbf{II}_B} \frac{\partial \mathbf{II}_B}{\partial \lambda_1} \right) \right) = \left( 1 + \frac{3}{\lambda_1^4 \lambda_2^2} \right) (\varphi_1 + \lambda_2^2 \varphi_2) + 2 \left( \lambda_1 - \frac{1}{\lambda_1^3 \lambda_2^2} \right)^2 (\varphi_{11} + 2\varphi_{12}\lambda_2^2 + \varphi_{22}\lambda_2^4) \geq 0. \end{aligned} \quad (18)$$

In this expression the relations (9)–(12) and

$$\frac{\partial \mathbf{I}_B}{\partial \lambda_1} = 2 \left( \lambda_1 - \frac{1}{\lambda_1^3 \lambda_2^2} \right), \quad \frac{\partial \mathbf{II}_B}{\partial \lambda_1} = 2 \left( \lambda_1 \lambda_2^2 - \frac{1}{\lambda_1^3} \right) = \lambda_2^2 \frac{\partial \mathbf{I}_B}{\partial \lambda_1} \quad (19)$$

are utilized. Since  $\lambda_1, \lambda_2 > 0$  holds, the gradient of the engineering stress  $T_{R11}$  for constant  $\lambda_2$  is non-negative. Unfortunately, we obtain no further insight from the second derivative  $\partial^2 T_{R11}/\partial \lambda_1^2$ . Analogously, in a diagram  $T_{R22}(\lambda_2)$  the ascent of the curve is non-negative.

## 2.2. Simple shear

A simple shear experiment is very difficult to handle. Nevertheless the resulting equations give a certain insight of the problem under investigation. For the motion  $\vec{\mathbf{x}} = \vec{\chi}_R(\vec{\mathbf{X}}, t) = (X_1 + \kappa X_2) \vec{\mathbf{e}}_1 + X_2 \vec{\mathbf{e}}_2 + X_3 \vec{\mathbf{e}}_3$  the deformation gradient  $\mathbf{F}$  as well as the left Cauchy–Green tensor  $\mathbf{B}$  and its inverse read:

$$\mathbf{F} = \vec{\mathbf{e}}_1 \otimes \vec{\mathbf{e}}_1 + \vec{\mathbf{e}}_2 \otimes \vec{\mathbf{e}}_2 + \vec{\mathbf{e}}_3 \otimes \vec{\mathbf{e}}_3 + \kappa \vec{\mathbf{e}}_1 \otimes \vec{\mathbf{e}}_2, \quad (20)$$

$$\mathbf{B} = \vec{\mathbf{e}}_1 \otimes \vec{\mathbf{e}}_1 + (1 + \kappa^2) \vec{\mathbf{e}}_2 \otimes \vec{\mathbf{e}}_2 + \vec{\mathbf{e}}_3 \otimes \vec{\mathbf{e}}_3 + \kappa (\vec{\mathbf{e}}_1 \otimes \vec{\mathbf{e}}_2 + \vec{\mathbf{e}}_2 \otimes \vec{\mathbf{e}}_1), \quad (21)$$

$$\mathbf{B}^{-1} = (1 + \kappa^2) \vec{\mathbf{e}}_1 \otimes \vec{\mathbf{e}}_1 - \kappa (\vec{\mathbf{e}}_1 \otimes \vec{\mathbf{e}}_2 + \vec{\mathbf{e}}_2 \otimes \vec{\mathbf{e}}_1) + \vec{\mathbf{e}}_2 \otimes \vec{\mathbf{e}}_2 + \vec{\mathbf{e}}_3 \otimes \vec{\mathbf{e}}_3. \quad (22)$$

The first and second invariant (2) and (3)

$$I_{\mathbf{B}} = \text{tr} \mathbf{B} = 3 + \kappa^2, \quad II_{\mathbf{B}} = \text{tr} \mathbf{B}^{-1} = 3 + \kappa^2 \quad (23)$$

lead to the strain-energy function  $\psi(I_{\mathbf{B}}, II_{\mathbf{B}}) = \sum_{i=0}^m \sum_{j=0}^n c_{ij} \kappa^{2(i+j)}$ , which is obviously non-negative for  $c_{ij} > 0$ . In the following, the shear force with respect to a change of the parameter  $\kappa$  is investigated. The shear stresses are calculable by use of Eqs. (6) and (21)–(22)

$$\sigma_{12} = \kappa(\varphi_1 + \varphi_2) \geq 0. \quad (24)$$

Since the stress coefficient  $T_{R12}$  of the first Piola–Kirchhoff tensor is equal to  $\sigma_{12}$ , the exterior tangential force  $F_t = \sigma_{12}A$  is non-negative. The gradient

$$\frac{\partial \sigma_{12}}{\partial \kappa} = \varphi_1 + \varphi_2 + 2\kappa^2(\varphi_{11} + 2\varphi_{12} + \varphi_{22}) \geq 0 \quad (25)$$

and its derivative with respect to  $\kappa$  always are non-negative:

$$\frac{\partial^2 \sigma_{12}}{\partial \kappa^2} = 6\kappa(\varphi_{11} + 2\varphi_{12} + \varphi_{22}) + 4\kappa^3(\varphi_{111} + 3\varphi_{112} + 3\varphi_{221} + \varphi_{222}) \geq 0. \quad (26)$$

Equality always holds in the undeformed state,  $\kappa = 0$ . In all other cases, the second derivative  $\partial^2 \sigma_{12} / \partial \kappa^2$  vanishes only for strain-energy functions which are merely linear in the first or the second invariant (Neo-Hooke and Mooney–Rivlin model as well as a model containing the term  $c_{01}(II_{\mathbf{B}} - 3)$ ).

### 2.3. Tension–torsion

In this subsection the analytical solution of the extension and torsion of a cylindrical body, which is a non-homogeneous deformation, is recalled. For this kind of deformation, based on the assumption of incompressibility, the motion is defined by  $r = \lambda^{-1/2}R$ ,  $\vartheta = \Theta + DZ$  and  $z = \lambda Z$ .  $(r, \vartheta, z)$  are the cylindrical coordinates in the current configuration representing the radial, the circumferential and the axial coordinates.  $(R, \Theta, Z)$  symbolize the cylindrical coordinates in the references configuration of a material point  $\vec{X}$ .  $\lambda$  denotes the stretch and  $D$  the twist.  $D$  represents an angle  $\alpha$  per undeformed length  $L_0$  and describes the relative distortion of the top and bottom planes with respect to the reference state,  $D = \alpha/L_0$ . The deformation gradient takes the form

$$\mathbf{F} = \text{GRAD} \vec{\chi}_R(\vec{X}, t) = \frac{\partial \vec{\chi}_R^k}{\partial X^L} \vec{g}_k \otimes \vec{G}^L = \begin{bmatrix} \lambda^{-1/2} & 0 & 0 \\ 0 & \lambda^{-1/2} & Dr \\ 0 & 0 & \lambda \end{bmatrix} \vec{e}_k \otimes \vec{E}_L \quad (27)$$

where the tangential vectors  $\vec{g}_1 = \vec{e}_r$ ,  $\vec{g}_2 = r\vec{e}_\vartheta$  and  $\vec{g}_3 = \vec{e}_z$  as well as the gradient vectors  $\vec{G}^1 = \vec{E}_R$ ,  $\vec{G}^2 = \frac{1}{R}\vec{E}_\vartheta$  and  $\vec{G}^3 = \vec{E}_Z$  are substituted by the unit vectors  $\vec{e}_k$ ,  $k = r, \vartheta, z$  and  $\vec{E}_L$ ,  $L = R, \Theta, Z$ . The left Cauchy–Green tensor  $\mathbf{B}$  and its inverse have the form

$$\mathbf{B} = \begin{bmatrix} \lambda^{-1} & 0 & 0 \\ 0 & \lambda^{-1} + (Dr)^2 & Dr\lambda \\ 0 & Dr\lambda & \lambda^2 \end{bmatrix} \vec{e}_k \otimes \vec{e}_l, \quad (28)$$

$$\mathbf{B}^{-1} = \begin{bmatrix} \lambda & 0 & 0 \\ 0 & \lambda & -Dr \\ 0 & -Dr & \lambda^{-2} + (Dr)^2\lambda^{-1} \end{bmatrix} \vec{e}_k \otimes \vec{e}_l \quad (29)$$

yielding the invariants

$$I_{\mathbf{B}} = \text{tr} \mathbf{B} = 2\lambda^{-1} + \lambda^2 + (Dr)^2, \quad II_{\mathbf{B}} = \text{tr} \mathbf{B}^{-1} = 2\lambda + \lambda^{-2} + (Dr)^2\lambda^{-1} \quad (30)$$

which are functions of the radius  $r$ .

Now, we look at the exterior quantities such as the normal force and the torque, measurable in experiments:

$$N = \int_A T_{zz} dA = 2\pi \int_0^{r_a} T_{zz} r dr, \quad M = \int_A T_{\vartheta z} r dA = 2\pi \int_0^{r_a} T_{\vartheta z} r^2 dr. \quad (31)$$

For example, in Hartmann (2001) it is shown that the normal force  $N$  and the torque  $M$  achieve the representation

$$N(\lambda, D) = 2\pi \int_0^{\lambda^{-1/2} R_a} \left( \left( \lambda^2 - \lambda^{-1} - \frac{(Dr)^2}{2} \right) \varphi_1 - \left( \lambda^{-2} - \lambda + (Dr)^2 \lambda^{-1} \right) \varphi_2 \right) r dr, \quad (32)$$

$$M(\lambda, D) = 2\pi D \int_0^{\lambda^{-1/2} R_a} (\varphi_1(r, \lambda, D) \lambda + \varphi_2(r, \lambda, D)) r^3 dr. \quad (33)$$

The functions  $\varphi_1$  and  $\varphi_2$  depend on the radius  $r$ , the stretch  $\lambda$  and the twist  $D$ ,  $\varphi_1(r, \lambda, D)$  and  $\varphi_2(r, \lambda, D)$ . This dependence is formally given by  $\hat{\varphi}_1(\lambda, (Dr)^2)$  and  $\hat{\varphi}_2(\lambda, (Dr)^2)$  caused by the invariants (30). In Eqs. (32) and (33) we have introduced the current exterior radius  $r_a$  by the reference radius of the specimen  $R_a$ ,  $r_a = \lambda^{-1/2} R_a$ . Furthermore, the boundary condition  $T_{rr}(r_a) = 0$  is exploited.

In the following two distinct investigations are performed. First, simple tension in the absence of torsion and, secondly, pure torsion are taken into consideration.

### 2.3.1. Simple tension

In the case of simple tension the normal force  $N$  can be derived, for example, by the biaxial tension problem for  $\lambda_1 = \lambda$  and  $\lambda_2 = \lambda^{-1/2}$ . Then the normal force (16) is known ( $N = N_1, N_2 = 0$ ):

$$\frac{N}{A_0} = (1 - \lambda^{-3})(\lambda \varphi_1 + \varphi_2). \quad (34)$$

We obtain the same result if we integrate Eq. (32) for  $D = 0$ ,  $A_0 = \pi R_a^2$ . The invariants (2) and (3) or (30) reduce to

$$I_B = \text{tr } \mathbf{B} = \lambda^2 + 2\lambda^{-1}, \quad II_B = \text{tr } \mathbf{B}^{-1} = 2\lambda + \lambda^{-2} \quad (35)$$

with the derivatives

$$\frac{dI_B}{d\lambda} = 2\lambda(1 - \lambda^{-3}) \quad \text{and} \quad \frac{dII_B}{d\lambda} = 2(1 - \lambda^{-3}) = \lambda^{-1} \frac{dI_B}{d\lambda}. \quad (36)$$

The function  $N(\lambda)$  has a non-negative gradient

$$\begin{aligned} \frac{1}{A_0} \frac{dN}{d\lambda} &= 3\lambda^{-4}(\lambda \varphi_1 + \varphi_2) + (1 - \lambda^{-3}) \left( \varphi_1 + \lambda \left( \varphi_{11} \frac{dI_B}{d\lambda} + \varphi_{12} \frac{dII_B}{d\lambda} \right) + \left( \varphi_{21} \frac{dI_B}{d\lambda} + \varphi_{22} \frac{dII_B}{d\lambda} \right) \right) \\ &= (1 + 2\lambda^{-3})\varphi_1 + 3\lambda^{-4}\varphi_2 + 2\lambda(1 - \lambda^{-3})^2(\lambda \varphi_{11} + 2\varphi_{12} + \lambda^{-1}\varphi_{22}) \geq 0 \end{aligned} \quad (37)$$

due to  $\lambda > 0$  and the properties (7)–(12), where we utilize derivatives (36). Thus, the function  $N(\lambda)$  increases monotonically for  $\lambda \rightarrow \infty$ . However, saddle points may occur. If we look at the gradient for  $\lambda = 1$ , Eq. (37) yields

$$\frac{1}{A_0} \frac{dN}{d\lambda} \Big|_{\lambda=1} = 6(c_{10} + c_{01}), \quad (38)$$

i.e. in a  $N(\lambda)$ -diagram the material parameters  $c_{10}$  and  $c_{01}$  are connected to the initial slope.

### 2.3.2. Pure torsion

In the subsequent analysis pure torsion is investigated ( $\lambda = 1$ ). The invariants (30) reduce to

$$I_B = \text{tr } \mathbf{B} = II_B = \text{tr } \mathbf{B}^{-1} = 3 + (Dr)^2 \quad (39)$$

which yields a derivative with respect to the twist  $D$  of

$$\frac{dI_B}{dD} = \frac{dII_B}{dD} = 2Dr^2. \quad (40)$$

Now, we examine the function  $M(D)$  and  $N(D)$  of Eqs. (32) and (33) for  $\lambda = 1$  and  $D \geq 0$ :

$$N(D) = -\pi D^2 \int_0^{R_a} (\varphi_1(r, D) + 2\varphi_2(r, D))r^3 dr, \quad (41)$$

$$M(D) = 2\pi D \int_0^{R_a} (\varphi_1(r, D) + \varphi_2(r, D))r^3 dr. \quad (42)$$

As a consequence of positive material parameters,  $c_{ij} > 0$ , we obtain the following behaviour: in a  $N(D)$  diagram the normal force always is negative (Poynting effect). The sign of the torque depends on the twist  $D$  and is negative for  $D < 0$  and positive for  $D > 0$  in the case of positive material parameters.

The gradients of the functions  $N(D)$  and  $M(D)$  are achieved by means of

$$\frac{\partial \varphi_1(r, D)}{\partial D} = 2Dr^2(\varphi_{11} + \varphi_{12}), \quad \frac{\partial \varphi_2(r, D)}{\partial D} = 2Dr^2(\varphi_{21} + \varphi_{22}), \quad (43)$$

and utilization of Eq. (40),

$$\frac{dN}{dD} = -2\pi D \int_0^{R_a} (\varphi_1 + 2\varphi_2)r^3 dr - \pi D^3 \int_0^{R_a} (\varphi_{11} + 3\varphi_{12} + 2\varphi_{22})r^5 dr, \quad (44)$$

$$\frac{dM}{dD} = 2\pi \int_0^{R_a} (\varphi_1 + \varphi_2)r^3 dr + 4\pi D^2 \int_0^{R_a} (\varphi_{11} + 2\varphi_{12} + \varphi_{22})r^5 dr. \quad (45)$$

Here,  $N'(D) \leq 0$  for  $D > 0$  and  $N'(D) \geq 0$  for  $D < 0$ . In contrast to this result the torque-twist curve  $M(D)$  always has a non-negative gradient. The second derivatives have the following signs:  $N''(D)$  is negative except for  $D = 0$ ,  $N''(D) \leq 0$  and  $M''(D) \leq 0$  for  $D < 0$  as well as  $M''(D) \geq 0$  for  $D > 0$ .  $M''(D) = 0$  holds for the undeformed state,  $D = 0$ , and for material models in which only the material parameters  $c_{01}$  and  $c_{10}$  occur.

Obviously, the gradient  $N'(D) = 0$  for  $D = 0$  holds. The gradient  $M'(0)$  is calculable from Eq. (45) to

$$\left. \frac{dM}{dD} \right|_{D=0} = \pi R_a^4(c_{10} + c_{01}) \quad (46)$$

and is connected to the material parameters  $c_{10}$  and  $c_{01}$ .

## 3. Further properties

The considerations of simple deformation processes (boundary value problems) are associated with the characteristics of the constitutive equations. An overview of the constitutive inequalities employed in the past to guarantee stability is given, for example, in Truesdell and Noll (1965, Sections 51–54), Wang and Truesdell (1973, Ch. 8) or Marsden and Hughes (1983, pp. 16ff). Although there are open questions with respect to the range of validity of the stability criteria and their effects, we examine the Baker–Ericksen inequality which is applicable in the case of incompressibility.

Baker and Ericksen (1954) – see especially Truesdell and Noll (1965, Section 53) – introduced some inequalities which imply the assumption that the greater principal stresses always occur in the direction of the greater principal stretches:

$$(\sigma_a - \sigma_b)(\lambda_a - \lambda_b) > 0 \quad \text{if } \lambda_a \neq \lambda_b \quad (47)$$

A sufficient condition for inequality (47) is represented by

$$\varphi_1 > 0 \quad \text{and} \quad \varphi_2 \geq 0. \quad (48)$$

The assumption of positive material parameters imply the positiveness of inequalities (48), see Eqs. (7) and (8). However, this is only a sufficient condition as well.

A further requirement corresponds to the behaviour of the strain-energy in extreme cases. In that case the influence of the pressure  $p$  is omitted. If one eigenvalue  $\lambda_i$  tends towards zero or infinity, the strain-energy function must become infinity:  $\lambda_i \rightarrow 0^+ \Rightarrow \psi \rightarrow +\infty$  or  $\lambda_i \rightarrow +\infty \Rightarrow \psi \rightarrow +\infty$ . This behaviour is obviously satisfied in view of Eq. (5) if the material parameters are all assumed to be positive.

Of course, the choice of positive material parameters is not a necessary condition for physically plausible curves. However, in the investigated examples they do not lead to any inconsistencies.

**Remark 1.** Another widely applied constitutive relation is due to Ogden (1972) based on the strain-energy function

$$\psi(\lambda_1, \lambda_2, \lambda_3) = \sum_{a=1}^m \frac{\mu_a}{\alpha_a} (\lambda_1^{\alpha_a} + \lambda_2^{\alpha_a} + \lambda_3^{\alpha_a} - 3), \quad (49)$$

det  $\mathbf{F} = \lambda_1 \lambda_2 \lambda_3 = 1$ , with the material parameters  $\mu_a$  and  $\alpha_a$ . In that article Hill's inequality to ensure stability is applied, which yields the inequality  $\mu_a \alpha_a > 0$  (no sum over  $a$ ) (Hill, 1970; Ogden, 1972). Similar to the proposal here, this inequality constraint is merely a sufficient condition satisfying the applied stability criteria. A discussion concerning the behaviour of the model as well as the identification of the material parameters are treated, for example, in Chadwick et al. (1977), Twizell and Ogden (1983), Ogden (1986), Benjeddou et al. (1993) and Gendy and Saleeb (2000).

#### 4. Identification using tension–torsion tests

In this section we study the identification of the material parameters  $c_{ij}$ . In the above-mentioned considerations the description of the deformation of homogeneous stress and strain states as well as the inhomogeneous deformation of the tension–torsion experiment yields a linear least-square problem with non-negative solution in the case of parameter identification, i.e. the material parameters are assumed to be non-negative. In order to achieve a systematic representation of all models in Table 1 and further probable models we convert the strain-energy function (1) to matrix notation for the case of tension–torsion tests:

$$\psi(\mathbf{I}_B, \mathbf{II}_B) = \underline{\mathbf{E}}^T(\mathbf{I}_B, \mathbf{II}_B)\underline{\mathbf{Y}}. \quad (50)$$

The superscript T denotes the transposition of a column vector. Column vectors are underlined once and matrices twice. The vector  $\underline{\mathbf{Y}} \in \mathbb{R}^{(m+1)(n+1)}$  contains the material parameters

$$\underline{\mathbf{Y}}^T = \{c_{00} \ c_{01} \ \dots \ c_{0n} \ c_{10} \ c_{11} \ \dots \ c_{1n} \ \dots \ c_{m0} \ \dots \ c_{mn}\} \quad (51)$$

and the vector  $\underline{\mathbf{E}}$  products of the invariants (30)

$$\underline{\mathbf{E}}^T(\mathbf{I}_B, \mathbf{II}_B) = \{a_0 b_0 \ a_0 b_1 \ \dots \ a_0 b_n \ a_1 b_0 \ \dots \ a_1 b_n \ \dots \ a_m b_0 \ \dots \ a_m b_n\}, \quad (52)$$

with

$$a_i = (\mathbf{I}_B - 3)^i \text{ for } i = 0, \dots, m \quad \text{and} \quad b_j = (\mathbf{II}_B - 3)^j \text{ for } j = 0, \dots, n. \quad (53)$$

The functions  $\varphi_1$  and  $\varphi_2$  lead to the representation

$$\varphi_1 = 2\mathbf{E}_1^T \mathbf{Y} \quad \text{and} \quad \varphi_2 = 2\mathbf{E}_2^T \mathbf{Y} \quad (54)$$

with  $\mathbf{E}_1 = \partial \mathbf{E} / \partial \mathbf{I}_B$  and  $\mathbf{E}_2 = \partial \mathbf{E} / \partial \mathbf{II}_B$ :

$$\mathbf{E}_1^T = \left\{ \hat{a}_0 b_0 \ \hat{a}_0 b_1 \ \dots \ \hat{a}_0 b_n \ \hat{a}_1 b_0 \ \dots \ \hat{a}_1 b_n \ \dots \ \hat{a}_m b_0 \ \dots \ \hat{a}_m b_n \right\}, \quad (55)$$

$$\mathbf{E}_2^T = \left\{ a_0 \hat{b}_0 \ a_0 \hat{b}_1 \ \dots \ a_0 \hat{b}_n \ a_1 \hat{b}_0 \ \dots \ a_1 \hat{b}_n \ \dots \ a_m \hat{b}_0 \ \dots \ a_m \hat{b}_n \right\}. \quad (56)$$

These vectors contain products of the coefficients (53) and their derivatives ( $\hat{a}_i = da_i / d\mathbf{I}_B$ ,  $\hat{b}_j = db_j / d\mathbf{II}_B$ ):

$$\hat{a}_i = \begin{cases} 0 & \text{for } i = 0, \\ i(\mathbf{I}_B - 3)^{i-1} & \text{for } i = 1, \dots, m. \end{cases} \quad \hat{b}_j = \begin{cases} 0 & \text{for } j = 0, \\ j(\mathbf{II}_B - 3)^{j-1} & \text{for } j = 1, \dots, n. \end{cases} \quad (57)$$

The normal force (32) and the torque (33) achieve the representation

$$N(\lambda, D) = \mathbf{Z}_N^T(\lambda, D) \mathbf{Y} \quad (58a)$$

$$M(\lambda, D) = \mathbf{Z}_M^T(\lambda, D) \mathbf{Y} \quad (58b)$$

with

$$\begin{aligned} \mathbf{Z}_N(\lambda, D) = 4\pi \int_0^{\lambda^{-1/2} R_a} & \left\{ \mathbf{E}_1(r, \lambda, D) \left( \lambda^2 - \lambda^{-1} - \frac{(Dr)^2}{2} \right) - \mathbf{E}_2(r, \lambda, D) \right. \\ & \left. \times \left( \lambda^{-2} - \lambda + (Dr)^2 \lambda^{-1} \right) \right\} r dr \end{aligned} \quad (59)$$

and

$$\mathbf{Z}_M(\lambda, D) = 4D\pi \int_0^{\lambda^{-1/2} R_a} \{ \lambda \mathbf{E}_1(r, \lambda, D) + \mathbf{E}_2(r, \lambda, D) \} r^3 dr. \quad (60)$$

Incorporating the different models of Table 1 is done as follows: the vectors  $\mathbf{Y} \in \mathbb{R}^{(m+1)(n+1)}$  and therefore  $\mathbf{Z}_N$  and  $\mathbf{Z}_M$ , i.e.  $\mathbf{E}_1$  and  $\mathbf{E}_2$ , are reduced to only those coefficients which are of interest. In other words, we depict the subset of material parameters in which we are interested. This subset is denoted by  $\tilde{\mathbf{Y}} \in \mathbb{R}^q$ .  $q$  is the number of material parameters,  $q = (m+1)(n+1) - c$ .  $c$  represents the number of material constants defined in advance by zero. A list of parameters  $m$ ,  $n$ ,  $q$  and  $c$  for the models of Table 1 is shown in Appendix A, Table 6. Thus the vectors  $\mathbf{Z}_N$ ,  $\mathbf{Z}_M$ ,  $\mathbf{E}_1$  and  $\mathbf{E}_2$  result in  $\tilde{\mathbf{Z}}_N$ ,  $\tilde{\mathbf{Z}}_M$ ,  $\tilde{\mathbf{E}}_1$  and  $\tilde{\mathbf{E}}_2$ . For example, the Mooney–Rivlin model with maximal exponents of the first and second invariant  $m = 1$  and  $n = 1$  leads to the vectors  $\mathbf{Y}^T = \{c_{00} \ c_{01} \ c_{10} \ c_{11}\}$  and  $\tilde{\mathbf{Y}}^T = \{c_{01} \ c_{10}\}$ , i.e.  $c = 2$  and thus  $q = 2$ . Therefore, the scalar products (58) need merely the reduced vectors  $\tilde{\mathbf{Z}}_N$  and  $\tilde{\mathbf{Z}}_M$  which have to integrate  $\tilde{\mathbf{E}}_1^T = \{\hat{a}_0 b_1 \ \hat{a}_1 b_0\}$  and  $\tilde{\mathbf{E}}_2^T = \{a_0 \hat{b}_1 \ a_1 \hat{b}_0\}$ . The coefficients of  $\tilde{\mathbf{Z}}_N$  and  $\tilde{\mathbf{Z}}_M$  are calculated in advance, i.e. they are integrated analytically for example with Mathematica (Wolfram, 1991). Now, the normal force and the torsional couple (58) obtain the form

$$N(\lambda, D) = \tilde{\mathbf{Z}}_N^T \tilde{\mathbf{Y}} \quad \text{and} \quad M(\lambda, D) = \tilde{\mathbf{Z}}_M^T \tilde{\mathbf{Y}}. \quad (61)$$

Now, we are interested in the incorporation of different experimental results. The number of test data (e.g.  $\lambda_i$ ,  $i = 1, \dots, n_k$ ) of each experiment is denoted by a number  $n_k$ .  $n_t$  defines the number of all experi-

ments. The maximum number of all test data of every experiment is symbolized by  $n_D$ ,  $n_D = \sum_{k=1}^{n_t} n_k$ . In the case of simple tension,  $D = 0$ , the stretches  $\lambda_i, i = 1, \dots, n_k$ , are prescribed and the normal forces  $\bar{N}_i, i = 1, \dots, n_k$ , are measured. The normal forces are assembled in a vector

$$\underline{d}_k^T = \{\bar{N}_{k1} \dots \bar{N}_{kn_k}\}. \quad (62)$$

For a pure torsion or combined tension–torsion experiment the stretches  $\lambda_i, i = 1, \dots, \hat{n}_k$ , and twists  $D_i, i = 1, \dots, \hat{n}_k$ , are prescribed. Here,  $n_k = 2\hat{n}_k$  holds. In this case the vector  $\underline{d}_k^T = \{\underline{d}_k^{N^T} \underline{d}_k^{M^T}\}$  contains the measured normal forces  $\underline{d}_k^{N^T} = \{\bar{N}_{k1} \dots \bar{N}_{k\hat{n}_k}\}$  and torques  $\underline{d}_k^{M^T} = \{\bar{M}_{k1} \dots \bar{M}_{k\hat{n}_k}\}$ . All test data  $\underline{d}_k, k = 1, \dots, n_t$ , is assembled in a long column vector:

$$\underline{d}^T = \{\underline{d}_1^T \dots \underline{d}_{n_t}^T\}, \quad \underline{d} \in \mathbb{R}^{n_D}. \quad (63)$$

In order to compare the experimental data  $\underline{d}$  with the simulated data we have to calculate for given simple tension test data  $\lambda_i, i = 1, \dots, n_k$ , the normal force  $N_i = N(\lambda_i, D_i = 0) = \underline{Z}_{Ni}^T(\lambda_i, D_i = 0)\underline{Y}$  by means of the reduced vector of Eq. (58a). These results are assembled in the vector

$$\begin{Bmatrix} N_{k1} \\ \vdots \\ N_{kn_k} \end{Bmatrix} = \underline{\underline{A}}_k \underline{\underline{Y}} \quad \text{with } \underline{\underline{A}}_k = \begin{bmatrix} \underline{\underline{Z}}_{Nk1}^T \\ \vdots \\ \underline{\underline{Z}}_{Nkn_k}^T \end{bmatrix} \in \mathbb{R}^{n_k \times q}. \quad (64)$$

On the other hand, in combined tension–torsion tests,  $\hat{n}_k$  simulated normal forces  $N_i = N(\lambda_i, D_i) = \underline{\underline{Z}}_{Ni}^T(\lambda_i, D_i)\underline{\underline{Y}}$  and  $\hat{n}_k$  simulated torques  $M_i = M(\lambda_i, D_i) = \underline{\underline{Z}}_{Mi}^T(\lambda_i, D_i)\underline{\underline{Y}}$  are assembled in

$$\begin{Bmatrix} N_{k1} \\ \vdots \\ N_{k\hat{n}_k} \\ M_{k1} \\ \vdots \\ M_{k\hat{n}_k} \end{Bmatrix} = \underline{\underline{A}}_k \underline{\underline{Y}} \quad \text{with } \underline{\underline{A}}_k = \begin{bmatrix} \underline{\underline{Z}}_{Nk1}^T \\ \vdots \\ \underline{\underline{Z}}_{Nk\hat{n}_k}^T \\ \underline{\underline{Z}}_{Mk1}^T \\ \vdots \\ \underline{\underline{Z}}_{Mk\hat{n}_k}^T \end{bmatrix} \in \mathbb{R}^{n_k \times q} \quad (65)$$

All these simulated values, namely (64) and (65) are assembled in the product  $\underline{\underline{A}} \underline{\underline{Y}}$  with

$$\underline{\underline{A}} = \begin{bmatrix} \underline{\underline{A}}_1 \\ \vdots \\ \underline{\underline{A}}_{n_t} \end{bmatrix}, \quad \underline{\underline{A}} \in \mathbb{R}^{n_D \times q}. \quad (66)$$

Usually, a least-square method is applied, where the norm of the residual  $\underline{r} = \underline{\underline{A}} \underline{\underline{Y}} - \underline{d}$  should be minimal

$$F(\underline{\underline{Y}}) = \frac{1}{2} \|\underline{r}\|_2^2 = \frac{1}{2} \underline{r}^T \underline{r} = \frac{1}{2} \|\underline{\underline{A}} \underline{\underline{Y}} - \underline{d}\|_2^2 \rightarrow \text{minimum} \quad (67)$$

with respect to the inequality constraints

$$\tilde{Y}_i \geq 0, \quad i = 1, \dots, q. \quad (68)$$

Hartmann (2001) proposed a weighting technique so that different physical quantities of different magnitude obtain better fitting results. According to Lawson and Hanson (1995) a row-scaling technique is utilized pre-multiplying the residual  $\underline{r}$  with a diagonal-matrix  $\underline{\underline{G}}$ ,  $\tilde{\underline{r}} = \underline{\underline{G}}\underline{r}$ . Then, we look for the solution of the modified extremal problem

$$\tilde{F}(\underline{\underline{Y}}) = \frac{1}{2} \|\underline{\underline{G}}\underline{r}\|_2^2 = \frac{1}{2} \|(\underline{\underline{G}}\underline{\underline{A}})\underline{\underline{Y}} - \underline{\underline{G}}\underline{d}\|_2^2 \rightarrow \text{minimum}, \quad \tilde{Y}_i \geq 0, \quad i = 1, \dots, q. \quad (69)$$

For simple tension tests coefficients

$$\alpha_k = \frac{1}{\max_{j=1,\dots,n_k} |\bar{N}_{kj}|} \quad (70)$$

and for combined tension–torsion tests

$$\alpha_k^N = \frac{1}{\max_{j=1,\dots,\hat{n}_k} |\bar{N}_{kj}|} \quad \text{and} \quad \alpha_k^M = \frac{1}{\max_{j=1,\dots,\hat{n}_k} |\bar{M}_{kj}|} \quad (71)$$

are chosen so that the row-scaling operator  $\underline{\underline{G}}$  acquires the form:

$$\underline{\underline{G}} = \begin{bmatrix} \underline{\underline{G}}_1 & & \\ & \ddots & \\ & & \underline{\underline{G}}_{n_t} \end{bmatrix} \quad \text{with} \quad \underline{\underline{G}}_k = \begin{cases} \alpha_k \underline{\underline{I}}_{(n_k)} & \text{simple tension,} \\ \alpha_k^N \underline{\underline{I}}_{(\hat{n}_k)} & \\ \alpha_k^M \underline{\underline{I}}_{(\hat{n}_k)} & \text{combined tension–torsion.} \end{cases} \quad (72)$$

The index next to the identity matrices  $\underline{\underline{I}}$  defines the dimension of the matrix,  $\underline{\underline{I}}_{(n_k)} \in \mathbb{R}^{n_k \times n_k}$ . With this weighting technique the maximal value of the torque and normal forces for each experiment is separately normed to one.

#### 4.1. Identification without constraints

In order to study the incorporation of the constraints (68) into the parameter estimation and the effects on realistic test data, some remarks have to be made with respect to the non-constraint problem. In Hartmann (2001) a systematic study of the linear least-square problem (67), especially (69), utilizing experimental test data of various tension–torsion tests published by Haupt and Sedlan (2001), is treated. In the latter work, a model of finite viscoelasticity is developed based on a proposal of Lubliner (1985) (see also Lion, 1997; Reese and Govindjee, 1998; and the literature cited there). In this model the stress-state is decomposed additively into equilibrium stresses, represented by an hyperelasticity relation and the rate-dependent overstresses. The equilibrium stress-state is achieved by certain relaxation processes. However, the proposed identification process here is not limited to just this kind of rubber.

In Hartmann (2001) the singular value decomposition (see e.g. Golub and van Loan, 1986, pp. 138ff or Kielbasinski and Schwetlick, 1988, pp. 240ff) is applied, which supplies further insight into the sensitivity of the problem under consideration. The singular values  $\sigma_k$  of the matrix  $\underline{\underline{A}}$  or  $\underline{\underline{G}}\underline{\underline{A}}$ , respectively, correspond to the eigenvalues  $v_k$  of the matrix  $\underline{\underline{C}} = \underline{\underline{A}}^T \underline{\underline{A}}$ ,  $\sigma_k^2 = v_k$ ,  $v_k > 0$ , and are used to define the condition number  $\kappa_2(\underline{\underline{A}}) = \sigma_1/\sigma_q$ . It has been shown that the weighting technique (69) with the row-scaling operator  $\underline{\underline{G}}$  of Eq. (72) is necessary to achieve considerably better results. Thus the condition number

$$\kappa_2(\underline{\underline{G}}\underline{\underline{A}}) = \sigma_1/\sigma_q \quad (73)$$

is taken into account in the investigations described below.  $\sigma_1$  symbolizes the maximal and  $\sigma_q$  the minimal singular value. Here no rank-deficiency of the matrix  $\underline{\underline{G}}\underline{\underline{A}}$  is assumed to occur so that  $q$  is equal to the rank of  $\underline{\underline{G}}\underline{\underline{A}}$ . The condition number is an indicator of the sensitivity of the resulting material parameters, i.e. for a high condition number the problem is extremely sensitive to perturbations of the test data and shows if nearly linear dependent columns of the matrix  $\underline{\underline{G}}\underline{\underline{A}}$  exist.

In Hartmann (2001) the parameter estimation is applied to the models of Table 1 incorporating a tension and a pure torsion test. The experimental data is shown in Figs. 1 and 2. These higher-order models approximate the material data inside the range of identification very well, which is evident in view of the residuals  $\tilde{r}$  in Table 2. Some of these models lead to negative material parameters calculated from the underlying least-square problem and show non-physical results outside the identification region.

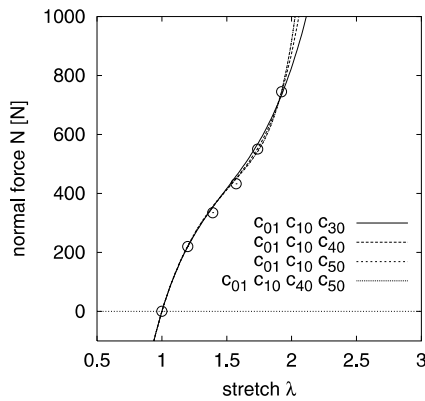


Fig. 1. Results of identification in simple tension test. Identification using simple tension and pure torsion (weighting technique used).

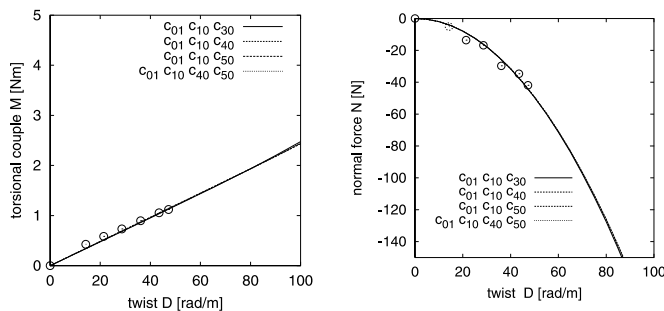


Fig. 2. Results of identification in pure torsion. Identification using simple tension and pure torsion (weighting technique used).

Table 2  
Condition number and residua for the tension and the torsion test using singular value decomposition

Models	$\tilde{r}$	$\kappa_2$
1	0.269	4.5
2	0.113	365
3	0.101	88700
4	0.226	9.25
5	0.688	1
6	0.116	238
7	0.106	15500
8	0.186	25.6
9	0.236	7.7
10	0.201	13.6
11	0.199	71.7
12	0.113	210

Furthermore, models 3 and 7 exhibit very large condition numbers leading to a very sensitive identification process.

#### 4.2. Identification using constraint conditions

In order to investigate the effect of positive material parameters, we consider the processes of simple tension and pure torsion shown in Figs. 1 and 2. The numerical method chosen is proposed by Lawson and Hanson (1995, Ch. 23) and the **FORTRAN**-code is obtainable from <http://www.netlib.org>. This method is specialized for the so-called NNLS, non-negative least-square problem.

##### 4.2.1. Application to simple tension and pure torsion

In Table 3 the constitutive models of Table 1 are presented again. Now, only non-negative material parameters are permitted. As a result of the identification process we see the following: only the framed parameters are identified with positive values. All other quantities are identified by the numerical method with zero. Except the Neo-Hookean model, all other models need the Mooney–Rivlin parameters  $c_{01}$  and  $c_{10}$ , which becomes clear in view of Eqs. (38) and (46). The material parameters  $c_{01}$  and  $c_{10}$  are necessary to represent the initial slopes of the simple tension process and the torsional couple versus twist curve. The higher-order terms identified are necessary to reproduce the curvature behaviour in the simple tensile test as well as the non-linear behaviour of the normal force versus twist curve in the pure torsion test.

It is interesting to note that the higher-order models only need one extra term with respect to the Mooney–Rivlin parameters (as a result of the applied numerical method), which is connected to the highest order of the first invariant  $I_B$ . Thus, we investigate the following models: first of all, all models should consist of the Mooney–Rivlin parameters  $c_{01}$  and  $c_{10}$  and further higher-order terms. Therefore, we choose the models containing  $c_{30}$  (model 13) or  $c_{40}$ , model number 14 (the model with the  $c_{50}$  term of Lion (1997) already exists, model 11). Furthermore, we have chosen a model with all material parameters up to the highest order 5 of the first invariant, i.e.  $c_{01}$ ,  $c_{10}$ ,  $c_{20}$ ,  $c_{30}$ ,  $c_{40}$ ,  $c_{50}$ . However, the identification procedure needs only the term  $c_{01}$ ,  $c_{10}$  as well as  $c_{40}$  and  $c_{50}$  (model 15). The other terms,  $c_{20}$  and  $c_{30}$ , are calculated to zero. These models are provided with the model numbers 13–15. In Table 6 of the appendix the models characterizing parameters are summarized.

Table 3  
Zero elements of the material models for identification with non-negative solution (framed coefficients are positive, non-framed coefficients are zero)

Models	Coefficients							
1	$c_{10}$	$c_{01}$						
2	$c_{10}$	$c_{01}$		$c_{11}$	$c_{20}$	$c_{02}$		
3	$c_{10}$	$c_{01}$		$c_{11}$	$c_{20}$	$c_{02}$	$c_{21}$	$c_{12}$
							$c_{30}$	$c_{03}$
4	$c_{10}$	$c_{01}$			$c_{20}$			
5	$c_{10}$							
6	$c_{10}$	$c_{01}$		$c_{11}$	$c_{20}$			$c_{30}$
7	$c_{10}$	$c_{01}$		$c_{11}$	$c_{20}$	$c_{02}$	$c_{21}$	$c_{30}$
								$c_{40}$
8	$c_{10}$	$c_{01}$			$c_{20}$			$c_{30}$
9	$c_{10}$	$c_{01}$		$c_{11}$				
10	$c_{10}$	$c_{01}$					$c_{22}$	
11	$c_{10}$	$c_{01}$						
12	$c_{10}$	$c_{01}$		$c_{11}$		$c_{02}$		$c_{30}$
								$c_{50}$

Table 4

Residuals, condition numbers and material parameters ( $N/m^2$ ) of particular models

Models	$\tilde{r}$	$\kappa_2$	$c_{01}$	$c_{10}$	$c_{30}$	$c_{40}$	$c_{50}$
13	0.206	16.8	$0.48660 \times 10^6$	$0.28478 \times 10^6$	$0.18718 \times 10^5$		
14	0.200	34.8	$0.47942 \times 10^6$	$0.29663 \times 10^6$		$0.81212 \times 10^4$	
11	0.199	71.7	$0.47333 \times 10^6$	$0.30579 \times 10^6$			$0.36698 \times 10^4$
15	0.199	95.5	$0.47366 \times 10^6$	$0.30530 \times 10^6$		$0.40259 \times 10^3$	$0.34894 \times 10^4$

Table 4 shows the results of the identification process. We see that the residuals  $\tilde{r}$  of the models decrease, i.e. the distance between the simulated data and the experimental data diminishes as the order of the first invariant increases. On the other hand, the condition number  $\kappa_2$  of definition (73) increases. Obviously, the material parameters  $c_{01}$  and  $c_{10}$  retain nearly constant values due to their physical meaning. In comparison to the unconstrained case, summarized in Table 2, the residuals deteriorate and the singular values have moderate magnitude.

**Remark 2.** The material parameters calculated in Table 4 are the same regardless of whether one uses the NNLS-algorithm or the singular value decomposition. Therefore the condition numbers in Table 4 are a result of the singular value decomposition proposed in the context of generalized polynomial-type hyperelasticity in Hartmann (2001).

Now, we look at the results of the identification process shown in Figs. 1 and 2. First of all, it is worth mentioning that the diagrams of simple tension, Fig. 1 and pure torsion, Fig. 2, show monotonic functions, even outside the identification region, which has been analytically proven in the previous sections. Secondly, the identification of these deformation processes using the weighting technique produces good results in Figs. 1 and 2 as well. Lastly, let us mention that models 11 and 13–15 of Table 4 behave almost identically.

In order to validate these models in a certain way, we simulate two further combined tension–torsion processes shown in Fig. 3 and compare the results with the experimental data of Haupt and Sedlan (2001) (for further details see Hartmann (2001)). In Fig. 4 we see that the models 11 and 13–15 produce good results for the rectangular path. Only the magnitude of the torsional couple during the first twist-controlled path is not reached. In the hourglass path this phenomena occurs as well, i.e. the torque is not represented as precisely as the normal forces. However, from a validation point of view, these results are satisfactory.

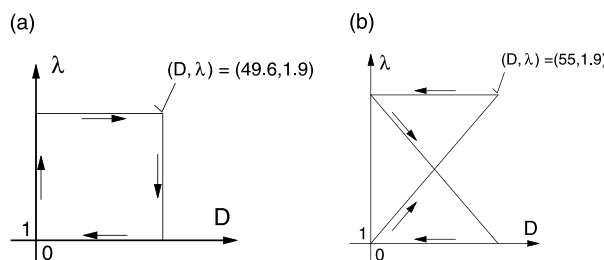


Fig. 3. Combined stretch and twist controlled tension–torsion test: (a) rectangular path (b) hourglass path.

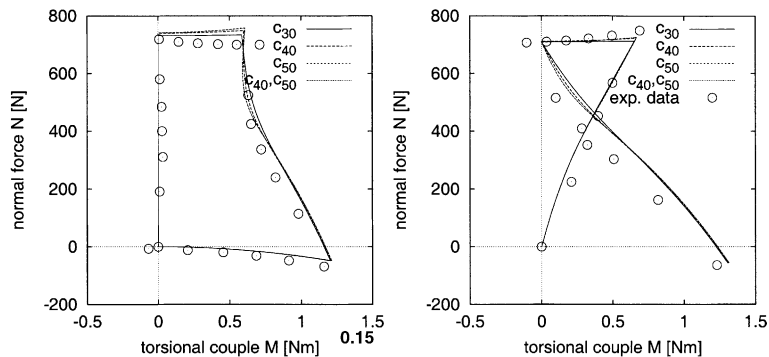


Fig. 4. Identification using simple tension and pure torsion tests (weighting technique used). Validation of models 11, 13–15 of Table 4.

Table 5

Residuals, condition numbers and material parameters ( $N/m^2$ ) of particular models. Incorporation of rectangular and hourglass path:  
(I) simple tension + pure torsion + rectangular path, (II) simple tension + pure torsion + rectangular path + hourglass path

	$\tilde{r}$	$\kappa_2$	$c_{01}$	$c_{10}$	$c_{30}$	$c_{40}$	$c_{50}$
<i>(I)</i>							
13	0.326	35.8	$0.49954 \times 10^6$	$0.26385 \times 10^6$	$0.18990 \times 10^5$		
14	0.321	75.2	$0.48186 \times 10^6$	$0.28844 \times 10^6$		$0.75628 \times 10^4$	
11	0.322	156	$0.47021 \times 10^6$	$0.30363 \times 10^6$			$0.32785 \times 10^4$
15	0.321	214	$0.47951 \times 10^6$	$0.29152 \times 10^6$		$0.59274 \times 10^4$	$0.71313 \times 10^3$
<i>(II)</i>							
13	0.382	43.1	$0.50405 \times 10^6$	$0.25354 \times 10^6$	$0.20560 \times 10^5$		
14	0.376	89.5	$0.48142 \times 10^6$	$0.28365 \times 10^6$		$0.81497 \times 10^4$	
11	0.377	184	$0.46643 \times 10^6$	$0.30230 \times 10^6$			$0.35358 \times 10^4$
15	0.376	255	$0.47965 \times 10^6$	$0.28587 \times 10^6$		$0.71103 \times 10^4$	$0.45403 \times 10^3$

#### 4.2.2. Application to several combined tension–torsion tests

In the following, in addition to the simple tension and pure torsion test, we also take into account the rectangular path and both the rectangular and hourglass paths of Fig. 3 and investigate the identification results. It is worth mentioning that the properties of non-zero elements of models 1–12 in Table 3 do not change if we incorporate the paths mentioned, i.e. the framed material parameters in Table 3 are the only positive quantities. Thus, we investigate models 11 and 13–15 again. Table 5 summarizes the results of both sets of parameter estimations.

In the first case (I) the experimental data of the simple tension, pure torsion and the rectangular path are taken into account. The material parameters  $c_{01}$  and  $c_{10}$  are close to the results of Table 4. The changes of the values of the models 11, 13 and 14 are small. Merely the higher-order terms of model 15 show a significant change between the underlying process of Tables 4 and 5(I). The additional incorporation of the hourglass experimental data behaves similarly, Table 5(II). Note that the residual becomes higher due to the increasing number of test data. The increase in the condition numbers indicates that the additional experiments give only a little further information. Since there is merely a small change between the incorporation of material data sets (I) and (II) we show only the results of set (II) in Fig. 5. Considering all test data hardly improves the results. This underpins the necessity of merely the simple tension and pure torsion test. Because of the sensitivity of model 15 we favour models 11, 13 and 14.

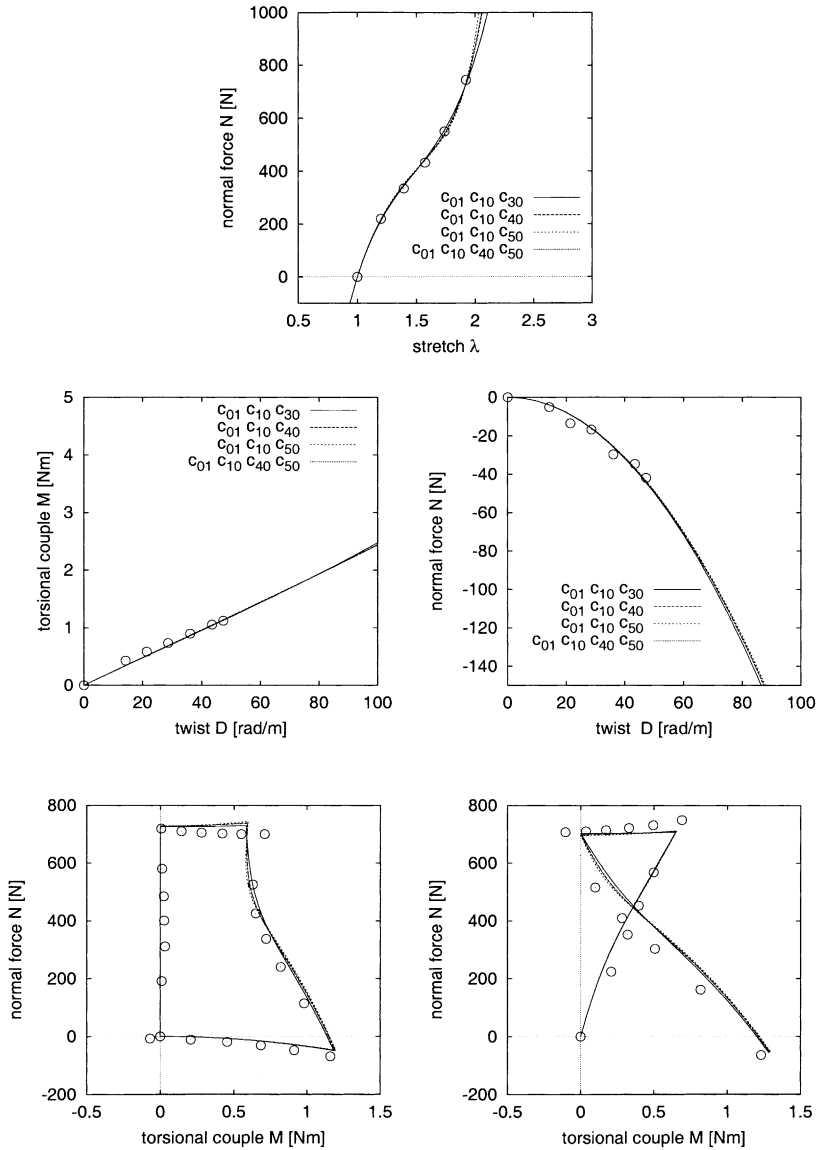


Fig. 5. Simulated tension–torsion tests with material parameters identified by a simple tension test, pure torsion test, rectangular path and hourglass.

**Remark 3.** There are some strain-energy functions where only the first invariant  $I_B$  is chosen. For example, the model of Arruda and Boyce (1993) has two positive, physically motivated material parameters for any order of the first invariant but leads to a non-linear least-square problem. Their model does not fit into Eq. (1). If we choose the model of Yeoh (1993) with the terms  $c_{10}$ ,  $c_{20}$  and  $c_{30}$  the identification method yields  $c_{10}$  as the only positive value.  $c_{20}$  and  $c_{30}$  are zero in order to satisfy the optimal solution of problem (69) with non-negative material parameters (in the article of Yeoh (1993) a negative material parameter is identified). This does not improve even if we choose the values  $c_{k0}$ ,  $k = 1, \dots, 5$ . Even in this case only the Neo–Hooke coefficient  $c_{10}$  is identified ( $c_{k0} = 0$ ,  $k = 2, \dots, 5$ ) (see also the discussion in Przybylo and Arruda, 1998).

## 5. Conclusion

In this article the assumption of merely positive material parameters in the context of incompressible hyperelastic relations of generalized polynomial-type is investigated. This assumption is a sufficient condition that the strain-energy function (1) is positive for every deformation process. However, it fulfills the requirement of the Baker–Ericksen inequality. Moreover, in several simple deformation processes the assumption of positive material parameters leads to monotonic functions of stress or forces under controlled stretches, shear angles or twists so that no non-physical behaviour can take place.

The identification of the material parameters using a least-square method applied to simple homogeneous deformation processes and the tension–torsion problem leads to an optimization problem with linear inequality constraints. The application of an identification procedure to some models of the literature incorporated in the generalized polynomial-type hyperelasticity leads to only a few essential material constants. The other parameters are identified by the numerical procedure with zeros. This reduces the number of necessary terms. However, the identification results may lead to a certain deterioration in the identification region but outside the identification region a non-physical behaviour is not recognizable. Furthermore, the sensitivity of the identification problem diminishes considerably.

## Acknowledgements

I would like to thank Professor Peter Haupt, Konstantin Sedlan and Dr. Lothar Schreiber for helpful discussions.

## Appendix A. Parameters of different models

Table 1 summarizes twelve models taken from the literature. The number of material parameters  $q$ , the order  $m$  and  $n$  of the first and second invariant  $I_B$  and  $II_B$  as well as the number  $c$  of prescribed material parameters, which are assumed to be zero in advance, are depicted in Table 6. Models 13–15 are investigated in Section 4.2.

## Appendix B. Behaviour of invariants

Since most textbooks on finite elasticity omit the proof, it will be shown that the terms in the parentheses of Eqs. (1) and (5) are positive. Since both invariants (2) and (4) have the structure  $x + y + (1/xy)$  with  $x > 0$  and  $y > 0$ , the parentheses of Eq. (5) read  $f(x, y) = x + y + (1/xy) - 3$ . The necessary condition for a minimum of this function is fulfilled for  $f_x = (\partial f / \partial x) = 0$  and  $f_y = (\partial f / \partial y) = 0$ . With  $f_x = 1 - (1/x^2y)$  and  $f_y = 1 - (1/xy^2)$  we arrive at  $x = y = 1$  for vanishing derivatives. In this case  $f(1, 1) = 0$  holds. Now, we have to show that the function  $f(x, y)$  fulfills the sufficient condition, i.e. the matrix

Table 6  
Coefficients of the investigated material models

Models	1	2	3	4	5	6	7	8	9	10	11	12	13	14	15
q	2	5	9	3	1	5	8	4	3	3	3	5	3	3	4
m	1	2	3	2	1	3	4	3	1	2	5	3	3	4	5
n	1	2	3	1	0	1	2	1	1	2	1	2	1	1	1
c	2	4	7	3	1	3	7	4	1	6	9	7	5	7	8

$$\begin{bmatrix} f_{xx} & f_{xy} \\ f_{yx} & f_{yy} \end{bmatrix} = \frac{1}{x^3 y^3} \begin{bmatrix} 2y^2 & xy \\ xy & 2x^2 \end{bmatrix}$$

has to be positive definite. The eigenvalues of this symmetric matrix (the positive coefficient in front of the matrix is omitted for brevity)

$$\sigma_{1,2} = x^2 + y^2 \pm \sqrt{(x^2 + y^2)^2 - 3x^2y^2} > 0$$

are real and obviously positive, i.e. the function  $f(x, y)$  is non-negative in any case ( $\lambda_1 > 0, \lambda_2 > 0$ ) and has a minimum for  $\lambda_1 = \lambda_2 = 1$ .

## References

Arruda, E.M., Boyce, M.C., 1993. A three-dimensional constitutive model for the large stretch behavior of rubber elastic materials. *Journal of the Mechanics and Physics of Solids* 41, 389–412.

Atkin, R.J., Fox, N., 1980. An introduction to the theory of elasticity. Longman, London.

Baker, M., Ericksen, J.L., 1954. Inequalities restricting the form of the stress–deformation relations for isotropic elastic solids and Reiner–Rivlin fluids. *Journal of the Washington Academy of Sciences* 44, 33–35.

Benjeddou, A., Jankovich, E., Hadhri, T., 1993. Determination of the parameters of Ogden's law using biaxial data and Levenberg–Marquardt–Fletcher algorithm. *Journal of Elastomers and Plastics* 25, 224–248.

Biderman, V.L., 1958. Rasceti na Procnost, pp. 40–87 (cited in Treloar, 1975).

Chadwick, P., Creasy, C.F.M., Hart, V.G., 1977. The deformation of rubber cylinders and tubes by rotation. *The Journal of the Australian Mathematical Society, Series B* 20, 62–96.

Gendy, A.S., Saleeb, A.F., 2000. Nonlinear material parameter estimation for characterizing hyperelastic large strain models. *Computational Mechanics* 25, 66–77.

Golub, G.H., van Loan, C.F., 1986. Matrix Computations. North Oxford Academic, London.

Hartmann, S., 2001. Numerical studies on the identification of the material parameters of Rivlin's hyperelasticity using tension–torsion tests. *Acta Mechanica*, in press.

Haupt, P., 2000. Continuum Mechanics and Theory of Materials. Springer, Berlin.

Haupt, P., Sedlan, K., 2001. Viscoplasticity of elastomeric materials. Experimental facts and constitutive modelling. *Archive of Applied Mechanics*, in press.

Haupt, P., Tsakmakis, C., 1996. Stress tensors associated with deformation tensors via duality. *Archive of Mechanics* 48, 347–384.

Hibbit, Karlsson, Sorenson, 1998. ABAQUS Theory Manual v.5.8.

Hill, R., 1970. Constitutive inequalities for isotropic elastic solids under finite strain. *Proceedings of the Royal Society of London Series A* 314, 457–472.

Isihara, A., Hashimoto, N., Tatibana, M., 1951. Statistical theory of rubber-like elasticity IV (two-dimensional stretching). *The Journal of Chemical Physics* 19, 1508–1512.

James, A.G., Green, A., Simpson, G.M., 1975. Strain energy functions of rubber. I. Characterization of gum vulcanizates. *Journal of Applied Polymer Science* 19, 2033–2058.

Johnson, A.R., Quigley, C.J., Mead, J.L., 1994. Large strain viscoelastic constitutive models for rubber, part I: formulations. *Rubber Chemistry and Technology* 67, 904–917.

Kao, B.G., Razgunas, L., 1986. On the determination of strain energy functions of rubber. *Proceedings of the Sixth International Conference on Vehicle Structural Mechanics*, 22–24 April Detroit Michigan, pp. 145–154.

Kielbasinski, A., Schwetlick, H., 1988. Numerische lineare Algebra. Harri Deutsch Verlag, Thun.

Lawson, C.L., Hanson, R.J., 1995. Solving Least Squares Problems. SIAM Society for Industrial and Applied Mathematics, Philadelphia.

Lion, A., 1997. On the large deformation behaviour of reinforced rubber at different temperatures. *Journal of the Mechanics and Physics of Solids* 45, 1805–1834.

Lubliner, J., 1985. A model of rubber viscoelasticity. *Mechanics Research Communications* 12, 93–99.

Marsden, J.E., Hughes, T.J.R., 1983. Mathematical Foundations of Elasticity. Prentice Hall, New Jersey.

Mooney, M., 1940. A theory of large elastic deformation. *Journal of Applied Physics* 11, 582–592.

Ogden, R.W., 1972. Large deformation isotropic elasticity – on the correlation of theory and experiment for incompressible rubberlike solids. *Proceedings of the Royal Society of London Series A* 326, 565–584.

Ogden, R.W., 1984. Non-Linear Elastic Deformations. Ellis Horwood, Chichester.

Ogden, R.W., 1986. Recent advances in the phenomenological theory of rubber elasticity. *Rubber Chemistry and Technology* 59, 361–383.

Przybylo, P.A., Arruda, E.M., 1998. Experimental investigations and numerical modeling of incompressible elastomers during non-homogeneous deformations. *Rubber Chemistry and Technology* 71, 730–749.

Reese, S., Govindjee, S., 1998. A theory of finite viscoelasticity and numerical aspects. *International Journal of Solids and Structures* 35, 3455–3482.

Rivlin, R.S., 1948. Large elastic deformations of isotropic materials I. Fundamental concepts. *Philosophical Transaction of the Royal Society of London Series A* 240, 459–490.

Rivlin, R.S., Saunders, D.W., 1951. Large elastic deformations of isotropic materials VII. Experiments on the deformation of rubber. *Philosophical Transaction of the Royal Society of London Series A* 243, 251–288.

Truesdell, C., Noll, W., 1965. The non-linear field theories of mechanics. In: S. Flügge (Ed.), *Encyclopedia of Physics*. Vol. III/3, Springer, Berlin.

Tschoegl, N.W., 1971. Constitutive equations for elastomers. *Journal of Polymer Science Part A-1* 9, 1959–1970.

Twizell, E.H., Ogden, R.W., 1983. Non-linear optimization of the material constants in Ogden's stress-deformation function for incompressible isotropic elastic materials. *The Journal of the Australian Mathematical Society Series B* 24, 424–434.

Wang, C.-C., Truesdell, C., 1973. *Introduction of Rational Elasticity*. Noordhoff, Leyden.

Wolfram, S., 1991. *Mathematica: a System for Doing Mathematics by Computer*. Second ed., Addison Wesley, Redwood City.

Yeoh, O.H., 1993. Some forms of strain energy function for rubber. *Rubber Chemistry and Technology* 66, 754–771.

## Further Reading

Treloar, L.R.G., 1975. *The Physics of Rubber Elasticity*. Third ed., Clarendon Press, Oxford.